Kitaev physics in the two-dimensional magnet $NiPSe_3$

Cheng Peng,[1,*,†] Sougata Mardanya,[2,*] Alexander N. Petsch,[1,3] Vineet Kumar Sharma,[2] Shuyi Li,[4] Chunjing Jia,[4]
Arun Bansil,[5,6] Sugata Chowdhury,[2] and Joshua J. Turner[1,‡]
[1]*Stanford Institute for Materials and Energy Sciences, SLAC National Accelerator Laboratory, Menlo Park, California 94025, USA*
[2]*Department of Physics and Astronomy, Howard University, Washington DC 20059, USA*
[3]*Linac Coherent Light Source, SLAC National Accelerator Laboratory, Menlo Park, California 94025, USA*
[4]*Department of Physics, University of Florida, Gainesville, Florida 32611, USA*
[5]*Department of Physics, Northeastern University, Boston, Massachusetts 02115, USA*
[6]*Quantum Materials and Sensing Institute, Northeastern University, Burlington, Massachusetts 01803, USA*

(Received 14 March 2024; revised 24 June 2024; accepted 1 August 2024; published 22 August 2024)

The Kitaev interaction, found in candidate materials such as α-$RuCl_3$, occurs through the metal (M)-ligand (X)-metal (M) paths of the edge-sharing octahedra because the large spin-orbit coupling (SOC) on the metal atoms activates directional spin interactions. Here, we show that even in $3d$ transition-metal compounds, where the SOC of the metal atom is negligible, heavy ligands can induce bond-dependent Kitaev interactions. In this work, we take as an example the $3d$ transition-metal chalcogenophosphate $NiPSe_3$ and show that the key is found in the presence of a sizable SOC on the Se p orbital, one which mediates the super-exchange between the nearest-neighbor Ni sites. Our study provides a pathway for engineering enhanced Kitaev interactions through the interplay of SOC strength, lattice distortions, and chemical substitutions.

DOI: 10.1103/PhysRevResearch.6.033206

The possibility of unconventional magnetism and exotic topological excitations continues to drive intense interest in quantum materials, especially in search of the illusive quantum spin liquid. Although there is no long-range order, the spins in this state of matter are entangled. The exactly solvable Kitaev model [1] has been shown to host the quantum spin liquid ground state, which arises from the bond-dependent anisotropic spin exchange in a honeycomb lattice and the associated magnetic frustration. The phase diagram [1] of the Kitaev model features both gapped and gapless spin-liquids, depending on the relative strengths of the various coupling parameters. While the original Kiteav model is for spin-$1/2$, numerical studies suggest that higher spins might also support the existence of quantum spin liquid states [2–5].

It has been a long journey searching for real candidate materials which realize this solvable theoretical model [6]. In this context, the quasi-two-dimensional (2D) layered compounds, such as $(Li, Na)_2IrO_3$ [7] and α-$RuCl_3$ [8], have been widely investigated. Magnetic compounds with $3d$ transition metals, including CrI_3 and $CrSiTe_3$, also could possibly carry the Kitaev interaction even though they contain spins higher than spin-$1/2$. Recent candidate materials also include $Na_2Co_2TeO_6$ and $Na_2Co_2SbO_6$, where magnetic Co-Te-O layers are separated by a nonmagnetic Na network, and Co atoms with pseudospin-$1/2$ make up the layered honeycomb structure.

The majority of the aforementioned candidate materials involve metal atoms (Ir, Ru, Co) with strong SOC in which the bond-dependent Kitaev spin interactions come into play when the nearest-neighbor electron hopping takes place through the metal (M)-ligand (X)-metal (M) paths of the structure through the edge-sharing octahedra [9–12]. Variations in the overlapping orbitals involved as one travels along different directions around the metal sites of the honeycomb lattice then results in anisotropic interactions, e.g., see Fig. 1 in Ref. [13] or Ref. [3], for instance. However, when the SOC is weak, as is typically the case in materials with $3d$ transition metals, the open question is if Kitaev physics can still emerge. For instance, if substantial SOC effects can emerge through heavy-atom ligands, combined with Hund's coupling in the p orbitals, a pathway should be possible to be created for producing bond-dependent Kitaev interactions [3]. It is clear that a deeper understanding in this area, and how Kitaev interactions can be activated and deactivated in magnetic materials, could provide a new basis for "engineering" candidate Kitaev materials.

In this Letter, we discuss the tuning of Kitaev interactions in the transition-metal chalcogenophosphates, a van der Waals family of magnets. For this purpose, we examine in-depth how bond-dependent anisotropic Kitaev spin interactions arise in $NiPSe_3$, and why these interactions are essentially absent in $NiPS_3$. Insight is thus gained into creating sizable Kitaev interaction terms in the Hamiltonian in Ni chalcogenophosphates, where these result when the Se p orbitals experience a strong

---

[*] These authors contributed equally to this work.
[†] Contact author: cpeng18@stanford.edu
[‡] Contact author: joshuat@slac.stanford.edu

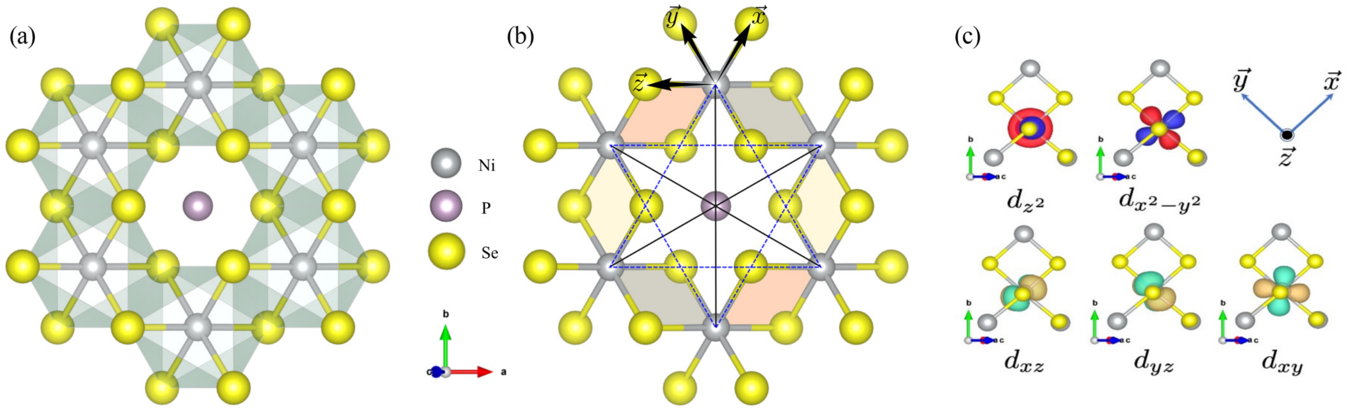

FIG. 1. (a) Lattice structure of a single $NiPSe_3$ layer viewed along $\mathbf{c}^*$, which is perpendicular to the *ab* plane. Ni atoms are positioned at the centers of the octahedral cages, and the edge-sharing octahedra form the honeycomb lattice of Ni. (b) The global coordinate axes $\{\vec{x}, \vec{y}, \vec{z}\}$ and the spin superexchange paths for nearest-neighbor Ni atoms are indicated by gray (*yz* plane), orange (*zx* plane), and yellow (*xy* plane) markers. The second- and third-neighbor Ni atoms are shown linked with blue dashed and black solid lines, respectively. (c) 3*d* orbitals of Ni atoms with fully filled t_{2g} orbitals in the bottom row and half-filled e_g orbitals in the top row, which are aligned in accord with the global coordinate axis $\{\vec{x}, \vec{y}, \vec{z}\}$.

SOC effect. The spin ground state of $NiPSe_3$ is stabilized primarily through the competition between the ferromagnetic nearest-neighbor coupling parameter J_1 and the antiferromagnetic third-neighbor Heisenberg coupling J_3, where effects of the lattice distortion lead to off-diagonal coupling terms. An analysis of the sizes of various coupling parameters in the Hamiltonian, in relation to the SOC strength, then allows us insight into favorable chemical substitutions for enhancing Kitaev physics in these materials.

The transition-metal chalcogenophosphates MPX_3 (TMCPs, where $M = \{\text{Mn, Fe, Ni, Co}\}$, and $X = \{\text{S, Se}\}$) form a family of van der Waals (vdW) magnetic materials [14,15]. Bulk $NiPX_3$ (X=$\{$S, Se$\}$) compounds, which is our focus here, have a monoclinic unit cell with space group $C2/m$ and point group C_{2h}. In the $NiPSe_3$ monolayer, the Ni atoms form a hexagonal structure with point group D_{3d}. Centers of the hexagons are occupied by phosphorus dimers [Fig. 1(a)] and the transition-metal atoms are enclosed within octahedral cages formed by nonmagnetic chalcogenide atoms that possess fully occupied *p* orbitals. Since $NiPX_3$ compounds are isostructural to α-$RuCl_3$ and CrI_3, their spin Hamiltonians can be constructed along similar lines if the effects of phosphorus dimers are neglected.

Due to the difficulty of growing fully Se-substituted single crystals, only a few experimental studies on $NiPSe_3$ appear in the literature [16–18]. Therefore, construction of an effective spin model for $NiPSe_3$ requires one to appeal to the spin models of other similar compounds as well as numerical simulations, although many features can be adapted from $NiPS_3$; see the Supplemental Material for details [19]. Aside from differences in the strength of the SOC, we hypothesize that the emergence of finite Kitaev spin interactions in $NiPSe_3$ is tied to the appearance of strong SOC on the ligand *p* orbitals. We show the efficacy of our hypothesis using second-order perturbation theory.

We will neglect minor trigonal distortions of the lattice and assume an orbital splitting of the t_{2g} and e_g orbitals by the octahedral crystal field, as illustrated in Fig. 1(c). The on-site Hamiltonian for the Ni sites on a single honeycomb layer is described by the Kanamori interaction [20]:

$$H_0 = U_{d(p)} \sum_{a} n_{a\uparrow} n_{a\downarrow} + \frac{U'_{d(p)}}{2} \sum_{a \neq b\sigma,\sigma'} n_{a\sigma} n_{b\sigma'} - \frac{J_{H_{d(p)}}}{2} \sum_{a \neq b,\sigma,\sigma'} c^{\dagger}_{a\sigma} c^{\dagger}_{b\sigma'} c_{b\sigma} c_{a\sigma'} + J_{H_{d(p)}} \sum_{a \neq b} c^{\dagger}_{a\uparrow} c^{\dagger}_{a\downarrow} c_{b\downarrow} c_{b\uparrow}. \tag{1}$$

Here $U_{d(p)}$ and $U'_{d(p)}$ are the intra and interorbital density-density interactions, respectively, and $J_{H_{d(p)}}$ is the Hund's coupling for the spin exchange and pair-hopping within the transition metal e_g (ligand *p*) orbitals. $n_{a(b)\sigma}$ is the density operator and $c^{\dagger}_{a(b)\sigma}$ ($c_{a(b)\sigma}$) is the creation (annihilation) operator acting on orbital *a* (*b*) and spin-σ. Here, *a* (*b*) is summed over all *d* orbitals on a transition metal site, or over all *p* orbitals on a ligand site. Importantly, for the on-site Hamiltonian of the ligand *p* orbitals, SOC is given by the term $H_{\text{SOC}} = \lambda_p \mathbf{L} \cdot \mathbf{S}$, where λ_p denotes the SOC strength and must be taken into account.

In our case, the Hund's coupling enforces a spin-1 half-filling configuration of the Ni e_g orbitals, while the *p* orbitals of the ligands are completely filled and do not contribute spins in our model. Thus, only the superexchange processes between the spins of neighboring $3d^8$-Ni sites contribute to our spin-1 model. The M-X-M superexchange is a fourth- or higher-order kinetic exchange process that involves hopping via the ligands. Note that ferromagnetic nearest-neighbor Heisenberg spin-1 coupling in $NiPX_3$ can only be understood through superexchange [21,22]. In contrast, direct exchange between the nearest-neighbor Ni sites is a second order kinetic exchange process that involves hopping between the transition-metal atoms without explicit involvement of the ligands, and therefore, it is antiferromagnetic and makes only a minor contribution.

The resulting spin model, if only the nearest-neighbor spin interactions are considered, is the well-known Kitaev-Heisenberg Hamiltonian:

$$\mathcal{H} = \sum_{\langle i,j\rangle} K^{\gamma} S_i^{\gamma} S_j^{\gamma} + J_1 \mathbf{S}_i \cdot \mathbf{S}_j + \Gamma\big(S_i^{\alpha} S_j^{\beta} + S_i^{\beta} S_j^{\alpha}\big) + \sum_{\langle i,j\rangle} \Gamma'\big(S_i^{\alpha} S_j^{\gamma} + S_i^{\gamma} S_j^{\alpha} + S_i^{\beta} S_j^{\gamma} + S_i^{\gamma} S_j^{\beta}\big). \tag{2}$$

In Fig. 1(b), the rotations $\{\alpha, \beta, \gamma\}$ are represented by $\{y, z, x\}$ (gray), $\{z, x, y\}$ (orange), and $\{x, y, z\}$ (yellow), respectively. The symmetric off-diagonal terms Γ and Γ' emerge from octahedral distortion effects [13].

We now discuss how electron hopping along the M-X-M path can be captured within the tight-binding formulation. By treating the tight-binding Hamiltonian as a perturbation to the on-site Hamiltonian, we can determine the coupling constants in the spin-1 model on the honeycomb lattice driven by superexchange processes. Building on the perturbation theory analysis from previous studies of $\mathrm{NiI_2}$ [3], $\mathrm{CrI_3}$ [13,23], and $\mathrm{NiPS_3}$ [21,23], we can then analyze $\mathrm{NiPSe_3}$. We produce the full derivation in the Supplemental Material [19], and outline the main results here. The resulting Kitaev coupling strength K^z associated, for example, with the yellow diamond in Fig. 1(b) can be simplified as

$$K^z \approx \frac{3}{2} \frac{t_{pd\sigma}^4 \lambda_p^2}{\big(2\Delta_{pd}^2 - \lambda_p \Delta_{pd} - \lambda_p^2\big)^2 (U_d - J_{H_d})}, \tag{3}$$

where Δ_{pd} is the charge transfer gap between the Ni d and Se p orbitals. $t_{pd\sigma}$ results from the Slater-Koster formulation [24] of the hopping integral between Ni $3d_{z^2}$ and Se p_z orbitals. Following suggestions for $\mathrm{NiI_2}$ [3] and $\mathrm{CrI_3}$ [13,23] in the literature, we assume that K^{γ} is scaled by λ_p^2 to lowest order. Note that in the ideal case, where a perfect cubic symmetry is preserved and the hopping integrals are accurately described by Slater-Koster parameters [24], the off-diagonal terms in Eq. (2) will vanish. We leave them here for realistic results that can eventually be matched to experiments.

Our main goal is to answer the question on whether the Kitaev spin interaction in $\mathrm{NiPSe_3}$ emerges simply from the replacement of S in $\mathrm{NiPS_3}$ by Se, i.e., to what extent can we view $\mathrm{NiPSe_3}$ to be a $\mathrm{NiPS_3}$-like system with stronger SOC residing on the ligand sites? An understanding of the mechanism responsible for producing Kitaev interactions could give insight into other novel effects in similar materials, such as topological magnon-phonon hybridization in $\mathrm{FePSe_3}$ [25]. We should keep in mind, however, that the strength of the Kitaev term K^{γ}, as well as the values of the Heisenberg coupling constants and off-diagonal terms, will likely deviate significantly from our perturbation-theory based analysis here when the lattice is distorted from the perfect octahedral structure. In fact, the Ni atoms sit in a local crystal-field with environment possessing D_3 symmetry, which already represents a slight deviation from the cubic symmetry O_h. Therefore, confirmation via numerical simulations using more realistic model parameters is still recommended.

TABLE I. Matrix components of our exchange Hamiltonian (in meV) featuring an effective spin-1 model, along with the nearest- and third-nearest-neighbor Heisenberg interactions J_1, J_3, and the bond-dependent Kitaev interaction parameter K^{γ} for the Ni sites within a single hexagonal layer. List of all Heisenberg couplings including the second-nearest-neighbor and interlayer interactions J_2, J_4 are given in the Supplemental Material [19]. Last row (marked with *) gives results for $\mathrm{NiPSe_3}$, where the SOC strength on the ligand Se is increased artificially.

	J_{xx}	J_{yy}	J_{zz}	J_{xy}	J_{yz}	J_{xz}
$\mathrm{NiPS_3}$	2.4822	2.4822	2.4832	0.0000	0.0000	0.0000
$\mathrm{NiPSe_3}$	1.2800	1.2400	1.3000	0.0180	0.0040	−0.0020
*$\mathrm{NiPSe_3}$	1.3988	1.2328	1.4708	0.0720	0.0120	−0.0080
	J_{α}	J_{β}	J_{γ}	K^{γ}	J_1	J_3
$\mathrm{NiPS_3}$	2.4822	2.4822	2.4832	−0.001	2.4852	−9.4798
$\mathrm{NiPSe_3}$	1.3003	1.2869	1.2328	0.0608	1.3040	−12.766
*$\mathrm{NiPSe_3}$	1.4718	1.4254	1.2052	0.2434	1.4928	−12.727

We follow the approach of Ref. [23] based on edge-sharing octahedra to extract the exchange Hamiltonian, which is a 3×3 matrix encompassing exchange couplings. We obtained fitted values of J_{α}, J_{β}, and J_{γ} using the global axes defined in Fig. 1(b). Notations of Ref. [23] are used for ease of comparison. Table I compares the K^{γ} term for $\mathrm{NiPS_3}$ and $\mathrm{NiPSe_3}$. Since S has negligible SOC in its p orbitals, K^{γ} for $\mathrm{NiPS_3}$ is also negligible. However, when S is replaced with Se and the SOC in the Se p orbitals is activated, K^{γ} becomes finite. To explore the importance of the ligand SOC in the K^{γ} term, we artificially increased the SOC strength in the ligand (third row of Table I, marked with *). Note that we considered the actual lattice structure, which includes lattice distortion by default. The strength of K^{γ} is seen to increase in proportion to that of λ_p^2, consistent with our perturbation theory analysis, see the Supplemental Material [19] for details. Notably, our conclusions here are in line with those of previous studies on $\mathrm{NiI_2}$ [3] and $\mathrm{CrI_3}$ [13,23].

We emphasize here that the enhancement of K^{γ} in this conventional Mott insulator $\mathrm{NiPSe_3}$ occurs because the Ni atoms form a hexagonal lattice with edge-sharing octahedra and the intervening ligand Se furthermore possesses strong SOC. This result suggests that the scaling of K^{γ} with λ_p^2 could be used more generally to control Kitaev interactions through chemical substitution of ligands in existing quantum magnets with similar lattice structures and superexchange interactions. By integrating this approach with machine learning models of structure predictions [26–34], it should be possible to significantly broaden the range of candidate Kitaev materials.

Interestingly, the strongest exchange term in Table I is seen to be the antiferromagnetic third-neighbor J_3, which increases with Se substitution (see the Supplemental Material [19] for the full list of Heisenberg couplings). This observation is in line with a previous experimental study that shows an increase in the Néel temperature by Se substitution in $\mathrm{NiP}X_3$ [16,18]. An antiferromagnetic J_3, which dominates in $\mathrm{NiPSe_3}$, however, is not conducive to realizing the spin liquid state, which requires a dominant K^{γ} term along with much smaller Heisenberg interactions [35]. The perspective [12] from perturbation theory shows that the energy scale of $J_3 \sim t_{pd\sigma}^4 t_{pp\sigma}^2 / \Delta_{pd}^4 (U_d - J_{H_d})$ is substantial because the $t_{pp\sigma}$ hopping integral between

Se p orbitals is sizable (see the Supplemental Material [19] for details on the hopping integrals). To suppress the long-range J_3 and obtain dominant nearest-neighbor couplings, it would be interesting to explore effects of chemical pressure and strain [21,36], as both ultimately cause lattice distortion and separate the overlapping Se p orbitals along the hopping path inducing J_3. This tuning of atomic distances could reduce the size of the hopping integral $t_{pp\sigma}$, and consequently enhance $|K^\gamma/J_3|$.

In conclusion, by examining the mechanism of Kitaev interactions within the transition-metal chalcogenophosphates and introducing this interaction to $NiPSe_3$, we hope to contribute an ingredient to the field of studying this family of compounds. This includes interpreting different experimental phenomena with or without this Kitaev term and studying the engineering of Kitaev interactions through chemical substitution on both the transition metal and phosphorus sites, thereby opening up a research channel for TMCPs.

This work is supported by the U.S. Department of Energy, Office of Science, Basic Energy Sciences under Award No. DE-SC0022216. This research used resources of the National Energy Research Scientific Computing Center , a DOE Office of Science User Facility supported by the Office of Science of the U.S. Department of Energy under Contract No. DE-AC02-05CH11231. This research at Howard University used Accelerate ACCESS PHYS220127 and PHYS2100073. We thank A. Feiguin, H.-C. Jiang, F. Liu, and Z. Chen for insightful discussions.

C.P. and J.J.T. instigated and designed this project. C.P. performed perturbation theory derivations, S.M. performed DFT+TB2J computations, A.P. provided experimental advice, V.K.S. performed DFT computations for various dopings, S.L. provided analytical advice, C.J., A.B., S.C., and J.J.T. supervised this project. C.P., A.P., S.M., and J.J.T. wrote the paper. All authors contributed to discussions and polishing of the manuscript.

[1] A. Kitaev, Anyons in an exactly solved model and beyond, Ann. Phys. **321**, 2 (2006).

[2] A. Koga, H. Tomishige, and J. Nasu, Ground-state and thermodynamic properties of an $S = 1$ Kitaev model, J. Phys. Soc. Jpn. **87**, 063703 (2018).

[3] P. P. Stavropoulos, D. Pereira, and H.-Y. Kee, Microscopic mechanism for a higher-spin Kitaev model, Phys. Rev. Lett. **123**, 037203 (2019).

[4] Y.-H. Chen, J. Genzor, Y. B. Kim, and Y.-J. Kao, Excitation spectrum of spin-1 Kitaev spin liquids, Phys. Rev. B **105**, L060403 (2022).

[5] X.-Y. Dong and D. N. Sheng, Spin-1 Kitaev-Heisenberg model on a honeycomb lattice, Phys. Rev. B **102**, 121102(R) (2020).

[6] M. Hermanns, I. Kimchi, and J. Knolle, Physics of the Kitaev model: Fractionalization, dynamic correlations, and material connections, Annu. Rev. Condens. Matter Phys. **9**, 17 (2018).

[7] B. J. Kim, H. Ohsumi, T. Komesu, S. Sakai, T. Morita, H. Takagi, and T. Arima, Phase-sensitive observation of a spin-orbital mott state in Sr_2IrO_4, Science **323**, 1329 (2009).

[8] A. Banerjee, J. Yan, J. Knolle, C. A. Bridges, M. B. Stone, M. D. Lumsden, D. G. Mandrus, D. A. Tennant, R. Moessner, and S. E. Nagler, Neutron scattering in the proximate quantum spin liquid α-$RuCl_3$, Science **356**, 1055 (2017).

[9] G. Jackeli and G. Khaliullin, Mott insulators in the strong spin-orbit coupling limit: From Heisenberg to a quantum compass and Kitaev models, Phys. Rev. Lett. **102**, 017205 (2009).

[10] J. G. Rau, E. Kin-Ho Lee, and H.-Y. Kee, Generic spin model for the honeycomb iridates beyond the Kitaev limit, Phys. Rev. Lett. **112**, 077204 (2014).

[11] C. Kim, H.-S. Kim, and J.-G. Park, Spin-orbital entangled state and realization of Kitaev physics in 3d cobalt compounds: A progress report, J. Phys.: Condens. Matter **34**, 023001 (2022).

[12] S. M. Winter, Magnetic couplings in edge-sharing high-spin d^7 compounds, J. Phys. Mater. **5**, 045003 (2022).

[13] P. P. Stavropoulos, X. Liu, and H.-Y. Kee, Magnetic anisotropy in spin-3/2 with heavy ligand in honeycomb Mott insulators: Application to CrI_3, Phys. Rev. Res. **3**, 013216 (2021).

[14] G. Ouvrard, R. Brec, and J. Rouxel, Structural determination of some MPS_3 layered phases (M = Mn, Fe, Co, Ni and Cd), Mater. Res. Bull. **20**, 1181 (1985).

[15] G. Le Flem, R. Brec, G. Ouvard, A. Louisy, and P. Segransan, Magnetic interactions in the layer compounds MPX_3 (M = Mn, Fe, Ni; X = S, Se), J. Phys. Chem. Solids **43**, 455 (1982).

[16] R. Basnet, K. M. Kotur, M. Rybak, C. Stephenson, S. Bishop, C. Autieri, M. Birowska, and J. Hu, Controlling magnetic exchange and anisotropy by nonmagnetic ligand substitution in layered MPX_3 (M = Ni, Mn; X = S, Se), Phys. Rev. Res. **4**, 023256 (2022).

[17] J.-Q. Yan, B. C. Sales, M. A. Susner, and M. A. McGuire, Flux growth in a horizontal configuration: An analog to vapor transport growth, Phys. Rev. Mater. **1**, 023402 (2017).

[18] H. Sun, L. Qiu, Y. Han, E. Yi, J. Li, M. Huo, C. Huang, H. Liu, M. Li, W. Wang, D.-X. Yao, B. A. Frandsen, B. Shen, Y. Hou, and M. Wang, Coexistence of zigzag antiferromagnetic order and superconductivity in compressed $NiPSe_3$, Mater. Today Phys. **36**, 101188 (2023).

[19] See Supplemental Material at http://link.aps.org/supplemental/10.1103/PhysRevResearch.6.033206 for complementrary results, and more analytical and numerical details.

[20] J. Kanamori, Electron correlation and ferromagnetism of transition metals, Prog. Theor. Phys. **30**, 275 (1963).

[21] C. Autieri, G. Cuono, C. Noce, M. Rybak, K. M. Kotur, C. E. Agrapidis, K. Wohlfeld, and M. Birowska, Limited ferromagnetic interactions in monolayers of MPS_3 (M = Mn and Ni), J. Phys. Chem. C **126**, 6791 (2022).

[22] S. Chaudhary, A. Ron, D. Hsieh, and G. Refael, Controlling ligand-mediated exchange interactions in periodically driven magnetic materials, arXiv:2009.00813.

[23] C. Xu, J. Feng, H. Xiang, and L. Bellaiche, Interplay between Kitaev interaction and single ion anisotropy in ferromagnetic

CrI_3 and $CrGeTe_3$ monolayers, npj Comput. Mater. **4**, 57 (2018).

[24] J. C. Slater and G. F. Koster, Simplified LCAO method for the periodic potential problem, Phys. Rev. **94**, 1498 (1954).

[25] J. Luo, S. Li, Z. Ye, R. Xu, H. Yan, J. Zhang, G. Ye, L. Chen, D. Hu, X. Teng, W. A. Smith, B. I. Yakobson, P. Dai, A. H. Nevidomskyy, R. He, and H. Zhu, Evidence for topological magnon–phonon hybridization in a 2D Antiferromagnet down to the monolayer limit, Nano Lett. **23**, 2023 (2023).

[26] R. E. A. Goodall, A. S. Parackal, F. A. Faber, R. Armiento, and A. A. Lee, Rapid discovery of stable materials by coordinate-free coarse graining, Sci. Adv. **8**, eabn4117 (2022).

[27] H. C. Wang, S. Botti, and M. A. L. Marques, Predicting stable crystalline compounds using chemical similarity, npj Comput. Mater. **7**, 12 (2021).

[28] H. Glawe, A. Sanna, E. K. U. Gross, and M. A. L. Marques, The optimal one dimensional periodic table: A modified Pettifor chemical scale from data mining, New J. Phys. **18**, 093011 (2016).

[29] G. Hautier, C. Fischer, V. Ehrlacher, A. Jain, and G. Ceder, Data mined ionic substitutions for the discovery of new compounds, Inorg. Chem. **50**, 656 (2011).

[30] R. Zhu, W. Nong, S. Yamazaki, and K. Hippalgaonkar, WyCryst: Wyckoff inorganic crystal generator framework, Matter (2024).

[31] M. Yang, KwangHwan Cho, A. Merchant, P. Abbeel, D. Schuurmans, I. Mordatch, and E. D. Cubuk, Scalable diffusion for materials generation, arXiv:2311.09235.

[32] C. Zeni, R. Pinsler, D. Zügner, A. Fowler, M. Horton, X. Fu, S. Shysheya, J. Crabbé, L. Sun, J. Smith, B. Nguyen, H. Schulz, S. Lewis, C.-W. Huang, Z. Lu, Y. Zhou, H. Yang, H. Hao, J. Li, R. Tomioka, and T. Xie, MatterGen: A generative model for inorganic materials design, arXiv:2312.03687.

[33] T. Xie, X. Fu, O.-E. Ganea, R. Barzilay, and T. Jaakkola, Crystal diffusion variational autoencoder for periodic material generation, arXiv:2110.06197.

[34] F. Liu, Z. Chen, T. Liu, Y. Lin, J. J. Turner, and C. Jia, Self-supervised generative models for crystal structures, iScience **27**, 110672 (2024).

[35] S. Trebst and C. Hickey, Kitaev materials, Phys. Rep. **950**, 1 (2022).

[36] A. V. Ushakov, D. A. Kukusta, A. N. Yaresko, and D. I. Khomskii, Magnetism of layered chromium sulfides $MCrS_2$ ($M =$ Li, Na, K, Ag, and Au): A first-principles study, Phys. Rev. B **87**, 014418 (2013).